Defence Research and Development Canada
Recherche et développement pour la défense Canada

DEFENCE R&D DÉFENSE

Limitations of Non-linear Dynamics in Predicting Sea Clutter Returns

Michael K. McDonald and Anthony Damini

Defence R&D Canada - Ottawa
TECHNICAL REPORT
DRDC Ottawa TR 2002-130
November 2002

Canada

Limitations of Non-linear Dynamics in Predicting Sea Clutter Returns

Michael K. McDonald and Anthony Damini
Aerospace Radar and Navigation Section

DEFENCE R&D CANADA - OTTAWA

TECHNICAL REPORT

DRDC Ottawa TR 2002-130

NOVEMBER 2002

Abstract

The ability to describe sea clutter returns via non-linear, and more specifically chaotic dynamics, is examined. It is shown that the commonly used chaotic invariant measures of correlation dimension and Lyapunov exponent are incapable of uniquely identifying chaotic processes and produce similar results for measured sea clutter returns and simulated stochastic processes. The potential existence of an underlying chaotic texture masked by stochastic overlying speckle is examined but found to be inconsistent with the measured properties of the measured sea clutter data. Finally, the performance of linear and non-linear predictors is tested against the real data but no improvement is found to exist for the non-linear predictor examined in this report with respect to linear prediction performance.

Résumé

Le présent rapport examine la possibilité de décrire le fouillis de mer en utilisant la dynamique des systèmes non linéaires et, plus précisément, chaotiques. On montre que les mesures invariantes chaotiques communément appliquées à la dimension de corrélation et à l'exposant de Lyapunov ne permettent pas d'identifier de façon unique les processus chaotiques et produisent des résultats semblables pour le fouillis de mer mesuré et les processus stochastiques simulés. L'existence possible d'une texture chaotique sous-jacente masquée par le speckle stochastique sus-jacent est également étudiée, mais elle s'avère également incompatible avec les propriétés des données de fouillis de mer mesurées. Enfin, l'efficacité prédictive des détecteurs linéaires et non linéaires est mise à l'essai en fonction des données réelles, mais aucune amélioration n'est constatée pour le prédicteur non linéaire examiné ici par rapport à l'efficacité de la prédiction linéaire.

This page intentionally left blank.

Executive summary

This report examines the ability to describe sea clutter returns via non-linear, and more specifically chaotic, dynamics. The study of radar detection of small targets in clutter has traditionally relied on the application of stochastic theory to the development of target detection schemes. In contrast to stochastic methods, it has recently been suggested that sea clutter returns can be modelled using chaos theory. Chaotic systems are non-linear dynamic systems with a relatively small number of degrees of freedoms.

The ultimate goal of applying chaotic theory to the sea clutter problem is to exploit its deterministic nature so as to develop accurate predictors for sea clutter returns. This ability to accurately predict sea clutter returns via a non-linear chaotic model should, in theory, result in substantial improvements in detection performance over that of stochastic models. This would improve the small target detection capabilities of radars such as the APS-506 on the CP-140 maritime patrol aircraft.

Past studies have shown that initial identifications of chaotic processes in low resolution sea clutter returns were, at best, highly ambiguous and indeed the returns seemed to be indistinguishable from stochastic processes. It was speculated that this shortcoming might be a result of the low resolution of early measured returns and that high resolution measurements would more accurately capture the underlying chaotic swell structure. In this report high resolution data (less than one metre) collected using the DRDC Ottawa XDM radar are analysed. It is shown that the commonly used chaotic invariant measures of correlation dimension and Lyapunov exponent are incapable of uniquely identifying chaotic processes and produce similar results for measured sea clutter returns and simulated stochastic processes. Additional tests examining the behaviour of the correlation function versus cut-off length for increasing embedding dimension indicates that sea clutter are consistent with a stochastic rather than chaotic process. The potential existence of an underlying chaotic texture masked by stochastic overlying speckle is also examined but again found to be inconsistent with the measured properties of measured sea clutter data. It is concluded that no evidence currently exists to support the existence of an underlying chaotic attractor in low resolution or high resolution sea clutter returns.

Finally, the prediction performance of linear and non-linear detectors is tested against the real data but no improvement is found to exist for the non-linear predictor examined in this report with respect to linear prediction performance.

McDonald, Michael K. 2002. Limitations of Non-linear Dynamics in Predicting Sea Clutter Returns. DRDC Ottawa TR 2002-130. Defence R&D Canada - Ottawa.

Sommaire

Le présent rapport examine la possibilité de décrire le fouillis de mer en utilisant la dynamique des systèmes non linéaires et, plus précisément, chaotiques. L'étude de la détection radar de petites cibles en présence de fouillis a par le passé reposé sur l'application de la théorie stochastique pour l'élaboration de plans de détection de cible. Suivant une approche opposée aux méthodes stochastiques, on a récemment suggéré que le fouillis de mer pourrait être modélisé à l'aide de la théorie du chaos. Les systèmes chaotiques sont des systèmes dynamiques non linéaires possédant un nombre relativement faible de degrés de liberté.

L'application de la théorie du chaos au problème du fouillis de mer vise en définitive à exploiter sa nature déterministe afin de définir des prédicteurs précis applicables au fouillis de mer. La capacité de prévoir exactement le fouillis de mer au moyen d'un modèle de chaos non linéaire devrait en principe permettre des améliorations sensibles de l'efficacité de la détection par rapport aux modèles stochastiques. On pourrait ainsi améliorer les capacités de détection de petites cibles au moyen de radars comme l'APS-506 utilisé à bord de l'aéronef de patrouille maritime CP-140.

Dans le présent rapport, des données à haute résolution (moins de un mètre) recueillies à l'aide du radar XDM du RDDC Ottawa ont été analysées. On montre que les mesures invariantes chaotiques communément appliquées à la dimension de corrélation et à l'exposant de Lyapunov ne permettent pas d'identifier de façon unique les processus chaotiques et produisent des résultats semblables pour le fouillis de mer mesuré et les processus stochastiques simulés. D'autres essais portant sur le comportement de la fonction de corrélation par rapport à la longueur de coupure pour l'augmentation de la dimension de prolongement indiquent que le fouillis de mer est compatible avec un processus stochastique plutôt qu'avec un processus chaotique. L'existence possible d'une texture chaotique sous-jacente masquée par le speckle stochastique sus-jacent est également étudiée, mais elle s'avère également incompatible avec les propriétés des données de fouillis de mer mesurées.

Enfin, l'efficacité prédictive des détecteurs linéaires et non linéaires est mise à l'essai en fonction des données réelles, mais aucune amélioration n'est constatée pour le prédicteur non linéaire examiné ici par rapport à l'efficacité de la prédiction linéaire.

McDonald, M.K. 2002. Limitations of Non-linear Dynamics in Predicting Sea Clutter Returns. DRDC Ottawa TR 2002-130. R&D pour la défense Canada - Ottawa.

Table of contents

This page intentionally left blank.

List of figures

This page intentionally left blank.

List of tables

This page intentionally left blank

1. Introduction

In 1990 Leung and Haykin [1] published a letter in which they first speculated that the dynamic behaviour of radar returns from sea clutter might be readily modeled through the use of chaotic dynamics. Following this initial letter, a series of subsequent papers [2,3,4,5] reported on measurements performed on collected sea clutter returns to identify characteristic invariants associated with chaotic processes. While many of these studies did produce results consistent with a chaotic process, namely a fractal dimension and at least one positive Lyapunov exponent, it remained unclear if the results were merely indicative of a coloured noise process rather than a chaotic process.

Unsworth et al. [6,7] re-examined the issue. They analysed real sea clutter returns and correlated random processes produced by simulation. By calculating the associated correlation dimension (D_c) using the maximum likelihood dimension (DML) estimate of Schouten et al. [8] and the embedding dimension (D_e) using the false nearest neighbours (*false_nearest*) method [9] they demonstrated that these methods produced estimates of correlation dimension and embedding dimension for both measured and simulated data sets that seemed consistent with chaotic processes; this despite the fact that the simulated sets were known to be random processes. This analysis was extended by calculating the correlation integral C(r) of Grassberger and Procaccia [10] whereby they observed that random processes could be distinguished from chaotic processes by the non-converging behaviour of the slopes of their C(r) versus cutoff length curves for increasing dimension. Their results were a strong indication that the DML and *false_nearest* algorithms used to calculate the chaotic invariants were not a reliable method of uniquely identifying chaotic processes and cast serious doubt on the existence of a chaotic attractor in the sea clutter returns.

All of the aforementioned studies focussed on the identification of chaos as the primary mechanism to explain the behaviour of sea clutter returns. While it has always been recognized that measured time series would contain measurement noise, more recently it has been recognized that dynamical noise may also play a major role [11]. Indeed, it has been postulated that sea clutter returns might be comprised of a random and chaotic component. Under this assumption the chaotic component would correspond primarily to the texture component while the speckle, or random, component would represent dynamic noise in the sea clutter returns. If the texture component is primarily chaotic in nature it may be possible to more accurately predict the fluctuations in texture using a non-linear predictor and thereby improve the detection performance to that more closely resembling ideal CFAR [12].

This paper examines the concept of an underlying chaotic texture by utilizing high resolution (i.e. sub-metre) sea clutter returns collected using the DRDC Ottawa Spotlight SAR eXploratory Development Model (XDM) airborne radar platform. Two aspects are examined.

1) The returns are analysed to determine the effectiveness of the chaotic characterizations and to examine the dependence of the invariant measures on the properties of the sea clutter returns. These results are compared with a simulated K-distributed time series possessing the same shape parameters and correlation characteristics as the real data.

2) The predictability of sea clutter returns is examined. The accuracy of predictions achieved using linear and non-linear predictors is quantified and compared.

2. Data Sets

The data analysed in this study was collected using the DRDC-Ottawa Spotlight SAR XDM radar system. This high resolution airborne radar system is capable of obtaining sub-metre measurements in spotlight, fixed squint and scanning modes. Table 1 summarizes the relevant operating parameters of the system.

Table 1. *Operating parameters of XDM radar.*

PARAMETER DESCRIPTION	PARAMETER VALUE
Frequency	9.5-10 GHz
Peak Power	500 kW
Azimuth Beamwidth	2.4°
Elevation Beamwidth	4°
Polarization	Horizontal-Horizontal
Sidelobes	-20 dB

Each data set is composed of 32768 records in which each record contains 1024 digitized samples of the range return echoes from each transmitted pulse. Due to abrupt changes of the front end gain setting in some of the data sets, it has been necessary to truncate these sets to remove sections in which the setting was adjusted. Table 2 summarizes the collection configuration of the data sets examined in this study.

Three different 'scanning' modes are employed in this study. During spotlight mode the antenna pointing angle and radar echo digitization are carefully controlled to ensure that the same geographic location remains centred in azimuth in range cell 512. In squint mode the radar squinting angle and radar echo digitization are held constant so that the sampled range cells migrate from pulse to pulse across the sea surface as the airborne platform moves. In sector mode the antenna is sectored across an azimuth width of 20° at a rate of approximately 6 rpm and the radar echo digitization is held constant. In sector mode the returns from a particular range cell correspond to a varying geographic location determined by the plane's motion and antenna azimuth within the sector.

In all cases the airborne platform is moving at a speed of approximately 75 m/s. The PRF associated with each data set is given in table 2 along with the approximate relationship of the viewing direction with respect to the sea swell.

Table 2. *Description of data sets.*

FILE NAME	PRF (HZ)	ANTENNA DEPRESSION ANGLE (^{O})	VIEWING ANGLE	RESOLUTION	MODE
472s17	692	4.54	Down-swell	<1m	Squint 85 degrees
472s19	715	8.97	Cross-swell	<1m	Squint 85 degrees
472s25	689	8.93	Up-swell	<1m	Squint 85 degrees
472s30	643	4.56	Cross-swell	<1m	Spotlighted
472s31	656	2.40	Cross-swell	<1m	Spotlighted
472s37	697	5.59	Down-swell	<1m	Spotlighted
472s38	674	2.39	Down-swell	<1m	Spotlighted
472s43	691	2.39	Cross-swell	<1m	Spotlighted
418s39	590	5.59	N/A	5m	Sectoring

Two types of times series are extracted:

1) Values are extracted from range bin 512. For the case of spotlight data this results in a time series of sea clutter returns from the same sea surface location separated by a sampling interval determined by the PRF of the data set. For the squint and sector modes the time series returns migrate across the sea surface according to the aircraft velocity and antenna azimuth within the sector. These time series are identified with ending ‘r512’.

2) A series of full range line returns (i.e. 1024 samples) are extracted from the spotlight mode data set and appended together to form a time series. These time series are identified with the ending ‘rl’.

The extracted time series are summarized in table 3. The shape parameter of each data set, as per the K distribution, was measured using the z log z method [13] and is also presented in table 3.

2.1 Generation of Simulated Data

As a cross check of the analysis of the chaotic invariants, a surrogate simulated time series is generated for each extracted real clutter time series. Each surrogate is composed of a correlated K distributed time series where the correlated gamma texture is generated per the approach of Tough and Ward [14].

The surrogate sets have the same approximate value of shape parameter and correlation as the corresponding measured data set. It is well known that the texture and speckle components of real sea clutter decorrelate on significantly different time scales; the underlying swell corresponding to the texure decorrelates over a time period on the order of seconds while the speckle decorrelates on the order of milliseconds. In this study, the texture correlation is extracted by calculating the squared power spectrum of the amplitude of the measured sea clutter return using an FFT and then box filtering the spectrum to remove all frequency components with a period of less than 0.1 seconds. The complex correlation of the speckle is obtained by performing a complex FFT and calculating the squared power spectrum. The resulting frequency domain correlation function for the speckle is not filtered as the contribution due to the texture component is minimal.

Table 3. *Extracted time series*

TIME SERIES	MODE	RECORD LENGTH	SHAPE PARAMETER (ν)	COMMENTS
472s17r512	Squint 85 degrees	16000	67.0	
472s19r512	Squint 85 degrees	16000	44.5	
472s25r512	Squint 85 degrees	25950	12.1	
472s30r512	Spotlight	21000	6.2	
472s31r512	Spotlight	20600	8.4	
472s37r512	Spotlight	16000	11.6	
472s38r512	Spotlight	16000	8.3	
472s43r512	Spotlight	16000	6.5	
418s39r512	Sector	32768		pdf is not K-distributed
472s30rl	Spotlight	26000	34.4	
472s31rl	Spotlight	26000	91.4	

3. Analysis of Chaotic Invariants

Two key invariant measures are examined for their ability to identify chaotic systems: the correlation dimension and the Lyapunov dimension (see for example [15]).

If sea clutter returns are to be well represented by a low dimensional dynamic system it is necessary that the correlation dimension of the system be finite and small. The correlation dimension is calculated for selected time series using the approach of Schouten et al. [8] as implemented within the *RRChaos* program [16] and per the method of Grassberger and Procaccia [10] as implemented within the d2 program of the Tisean package [17].

In addition to a finite fractal correlation dimension at least one of the measured Lyapunov dimensions must be positive to allow for the expanding flow associated with a chaotic attractor [15]. As a precursor to calculating the maximum Lyapunov component it is necessary to determine the appropriate embedding dimension (D_e), embedding delay and Theiler window. The significance of the first two of these parameters is briefly discussed in the following sections on non-linear prediction; the interested reader is referred to Parker et al. [15] for a more complete discussion. These parameters are calculated using routines *false_nearest*, *mutual* and *stp*, respectively, of the Tisean chaotic analysis package [17]. The calculated parameters for the examined time series are given in table 4.

The maximum Lyapunov exponent for each time series was calculated using the Tisean function *lyap_k* based on the approach of Kantz [18]. This function outputs the logarithm of the stretching factor versus time step; when an appropriate range of time steps is reached the slope of the output will become linear and equal to the maximum Lyapunov exponent.

3.1 Results of Chaotic Analysis

Table 5 lists the correlation dimension (D_c) calculated for each of the data sets per the DML algorithm. The results for the corresponding simulated K-distributed sets are also shown. Both results are summarized in the histogram in Figure 1. The most noticeable result is that both the measured and simulated sets present very similar ranges of calculated Dc. In all cases the maximum possible normalized embedding dimension was used to minimize the effect of noise on the calculation [8]. Comparisons of values with lower normalized embedding dimensions show that good convergence has been obtained.

It can be observed from figure 2 that a weak positive correlation exists between the shape parameter and D_c for both the measured and simulated data sets.

Table 4. *Extracted time series*

TIME SERIES	DELAY FROM MEAS. DATA	DELAY FROM SIMULATED DATA	D_e FROM MEAS. DATA	D_e FROM SIMULATED DATA	THEILER WINDOW FROM MEAS. DATA	THEILER WINDOW FROM SIMULATED DATA
472s17r512	3	3	4	6	18	18
472s19r512	5	5	5	6	20	10
472s25r512	3	3	6	6	18	24
472s30r512	2	3	6	6	20	40
472s31r512	2	2	6	5	18	30
472s37r512	5	2	6	4	20	34
472s38r512	4	1	4	4	20	34
472s43r512	9	2	6	6	25	30
472s30rl	7	Not examined	5	Not examined	31	Not examined
472s31rl	4	Not examined	7	Not examined	18	Not examined

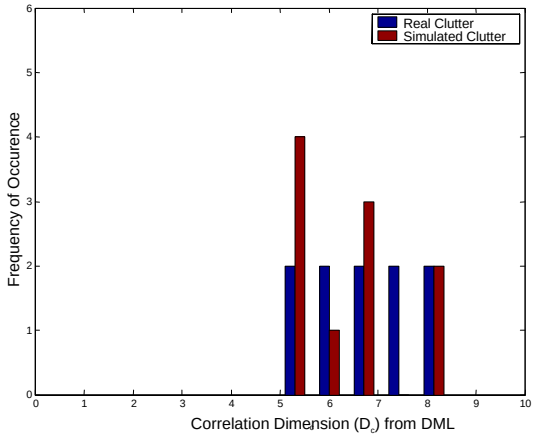

Figure 1. *Histograms of correlation dimensions calculated for non filtered, measured and simulated data.*

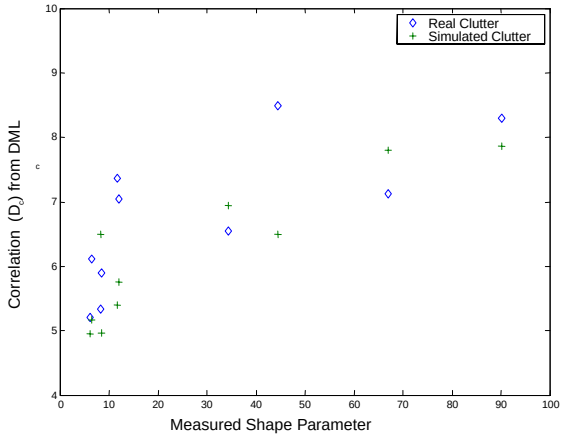

Figure 2. *Correlation dimensions from DML calculation versus shape parameter.*

Figure 3 demonstrates the results of applying the Grassberger and Procaccia method to real time series 472s30r512. Each curve in figure 3 represents the calculation of log(C(r)) versus cut-off length for a different embedding dimension. If the time series is chaotic a sufficiently large embedding dimension will be reached at which point the slopes of the linear section of the curves will become constant and equal to the correlation dimension for small values of D_c. It is readily apparent that this stabilization of the slope value does not occur for small values of D_c. As argued by Unsworth et al. [6] this final test effectively shows that the real sea clutter returns do not, in fact, possess a small finite correlation dimension. Although not shown for brevity, the same non-converging behaviour is observed for all the time series examined.

The maximum Lyapunov dimension was next analysed. The logarithm of the stretching factor is output by the *lyap_k* program and the slope of the linear section gives the Lyapunov exponent. For both real and surrogate data sets the plotted slopes are quite noisy and in some cases highly oscillatory. Kantz [18] states that the oscillatory nature of the response is not a problem as long as a clear linear trend is observed. Nevertheless, the combination of noise and oscillations make it difficult to accurately quantify the magnitude of the calculated slopes although in all cases it is apparent that a positive slope, and therefore a positive Lyapunov exponent, is present. However, further examination of the results reveals that the same behaviour is seen for the simulated stochastic. It can only be concluded that a determination of chaos is ambiguous at best from an examination of the maximum Lyapunov exponent of the measured time series. Table 5 summarizes the approximate Lyapunov exponent for each time series considered as determined from the average of 10-15 lines corresponding to a range of length scales that give linear results.

Table 5. *Extracted time series*

TIME SERIES	D_C FROM MEAS. DATA	D_C FROM SIMULATED DATA	MAXIMUM LYAPUNOV EXPONENT FROM MEAS. DATA	MAXIMUM LYAPUNOV EXPONENT FROM SIMULATED DATA
472s17r512	5.4	8.0	0.003	0.005
472s19r512	4.9	6.5	0.012	0.003
472s25r512	5.2	5.8	0.005	0.006
472s30r512	5.2	4.9	0.004	0.007
472s31r512	5.9	5.0	0.008	0.001
472s37r512	7.4	5.4	0.004	0.001
472s38r512	5.3	6.5	0.003	0.001
472s43r512	6.1	5.2	0.003	0.003
472s30rl	6.5	6.9	Not examined	Not examined
472s31rl	8.3	7.9	Not examined	Not examined

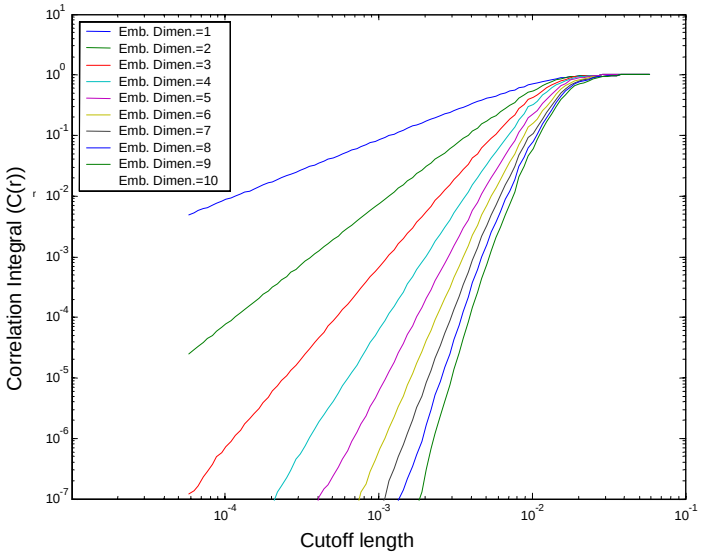

Figure 3. *Log-log plot of correlation integral (C(r)) versus cutoff length for increasing embedding dimension for time series 472s30r512.*

3.2 Filtered Data Sets

The above analysis would seem to preclude a chaotic interpretation, however it is unclear to what extent this could be the result of a strong dynamical noise component masking the underlying chaotic signature. To examine this effect it is necessary to remove or minimize the influence of the noise on the calculations.

As discussed in the introduction, it is speculated that the chaotic component of the signal returns may in fact be more strongly associated with the underlying texture, or in physical terms the swell component of the ocean surface. The swell modulates the mean power level of the random speckle component. It is well known that the K-distribution is a good fit to many sea clutter returns (see for example [12,19]). Under this construction the mean power level of the speckle is indeed equal to underlying texture, t, and the variance associated with the Rayleigh distributed speckle is given by $\sigma^2_{Rayleigh} = t - \frac{t\pi}{4}$. If t is assumed to represent the signal and $\sigma_{Rayleigh}$ the noise, then very poor signal to noise ratios can result. If the assumption of chaotic texture and stochastic speckle is valid it should be possible to significantly reduce the contribution of speckle to the overall signal by exploiting the much different correlation times of the two components. The typical correlation times of speckle

are on the order of ms seconds while that of texture is on the order of seconds. In this section, a series of low pass filters are applied to the data to progressively dampen the speckle response.

Three filters are used:

1) A 3 sample length box filter convolved with the time series.
2) A 9 sample length box filter convolved with the time series.
3) A 10 hz bandwidth box filter applied in the frequency domain.

To gain a qualitative understanding of the effect of filtering on a process in which an underlying slowly varying chaotic component modulates a stochastic process we first create a similar process by modulating a uniformly distributed random process using a chaotic Duffing equation.

The Duffing process is specified by

$$\frac{d^2y}{dt} = -\delta\frac{dy}{dt} + y - y^3 + \gamma\cos(\omega t),$$

where δ is the damping inherent in the system, and ω and γ are the angular frequency and amplitude, respectively, of the forcing term. The chaotic output used in this study is shown in figure 4a. The rand function of Matlab is used to generate a speckle vector that is multiplied by the output shown in figure 4a. The modulated output is shown in figure 4b. The effect of applying a convolving 39 element box filter with the Duffing modulated data is shown in figure 4c.

Table 6 summarizes the results of applying the DML calculation to each of the Duffing modulated data sets of figure 4. It is readily seen that the estimates produced by all sets are finite and of low dimension. The calculated values more closely approach that of the pure Duffing measurement after the low pass filter is applied but even for the unfiltered set the error is not large. Perhaps even more important are the results of the d2 calculation on each of the data sets as shown in figure 5. It is clearly evident that for the pure Duffing case (i.e. no speckle) the slopes of the curves stabilize for increased but small embedding dimension. This result is not observed for the unfiltered set but becomes more apparent as the filtering is increased. This qualitative example suggests that the speckle component can indeed hide the underlying chaotic behaviour in the d2 analysis. However, if the texture of the measured data sets is well modeled by a chaotic process it will produce finite, low dimensional estimates of correlation dimension via the DML method, and, in addition, the output of the d2 analysis will converge to constant slopes as filtering is increased. It should be noted that there is a limit to the improvement that can be obtained by filtering as it is impossible to limit the effects of filtering to the speckle component and, at some point, the increased filtering could seriously alter the underlying chaotic structure.

Figure 6 presents the histograms of the correlation dimension for each of the sets. Table 7 summarizes the results of the DML calculation on the sets. A general decrease in the mean and variance of D_c is observed as the filtering is increased which would seem to support the

concept that the speckle was masking the underlying chaotic texture, however the observed trend is present for both the measured and the simulated stochastic sets. This suggests that the observed behaviour might instead represent a negative relationship between the correlation of the processes and the calculated D_c, i.e. as the correlation of the time series is increased through high pass filtering, the measured D_c decreases.

To clarify the situation the output of the d2 calculation is analysed using measured data. Figure 7 displays the results of performing the d2 analysis on measured data set hdrs30r512. It is clearly evident from the figure that there is no convergence in the slope of the curves as the embedding dimension is increased. The results for the other data sets are not shown for the sake of brevity but display a similar behaviour. Thus, after examining the different measured invariants (D_c from DML and Lyapunov exponents) of the sea clutter sets it is concluded that, at most, they provide an ambiguous identification of a chaotic signal in that they display the same behaviour for measured and simulated stochastic sets. Additionally, the d2 calculation is clearly inconsistent with small finite dimension chaotic processes. Therefore, measured data sets would appear to be indistinguishable from similar stochastic processes.

Table 6.*Correlation Dimension Duffing modulated processes.*

FILE NAME	NO SPECKLE D_C	NO FILTER	39 POINT BOX FILTER
Duffing Process	2.3	3.1	2.2

(a)

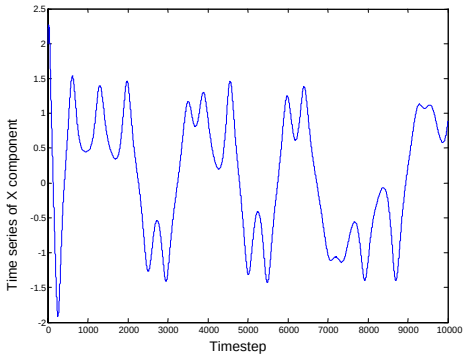

(b)

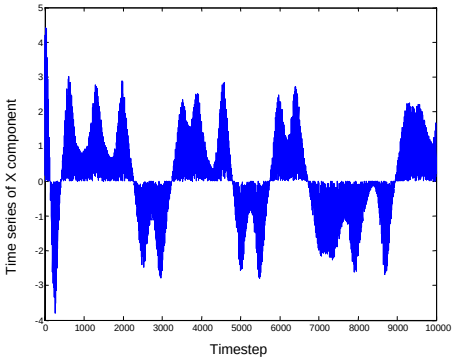

(c)

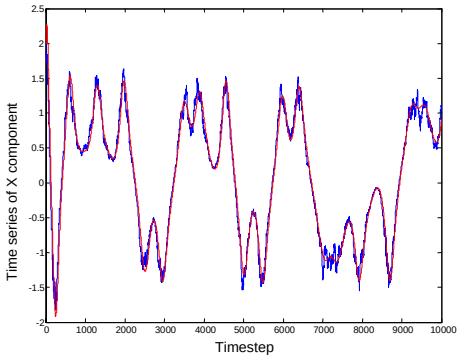

Figure 4: *Chaotic behaviour of Duffing's equation δ = 0.25, γ=0.3, ω=1.0 (a) No speckle (b) Speckle modulated by Duffing output. (c) Speckle modulated by Duffing output and a 39 sample box filter applied. Filtered signal in blue, no speckle signal in red.*

(a)

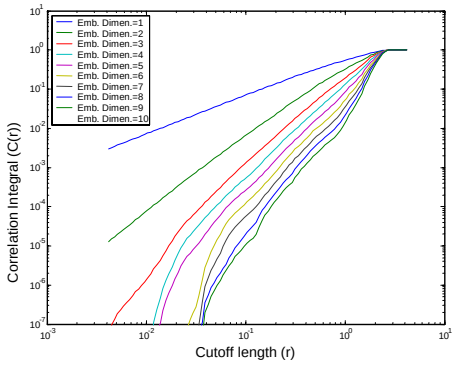

(b)

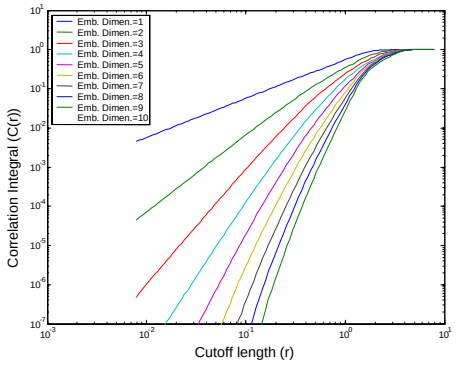

(c)

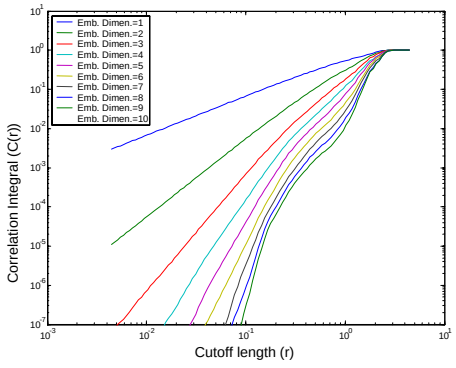

Figure 5: *Plot of log(C(r)) versus log(cutoff length) for a) pure Duffing output, b) uniform random process modulated by Duffing output, c) uniform random process modulated by Duffing output with 39 element box filter applied .*

(a)

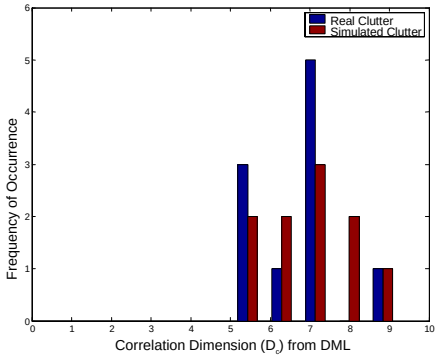

(b)

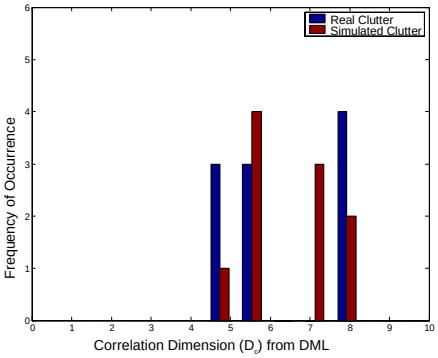

(c)

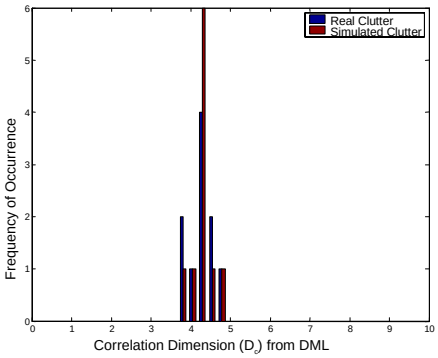

Figure 6: *Histograms of correlation dimensions calculated for measured and simulated data with a) 3 element box filter applied, b) 9 element box filter applied c) 10 hz box filter in frequency domain.*

(a)

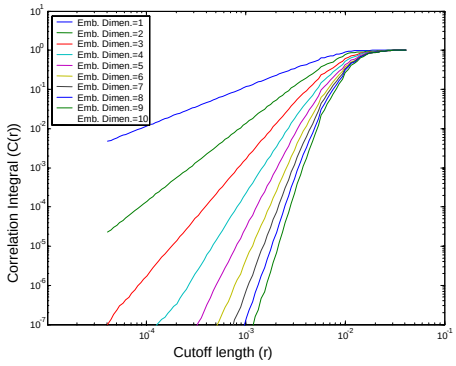

(b)

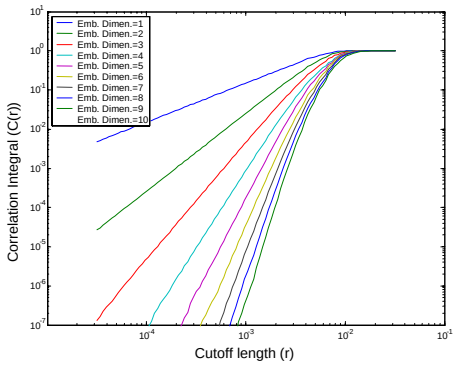

(c)

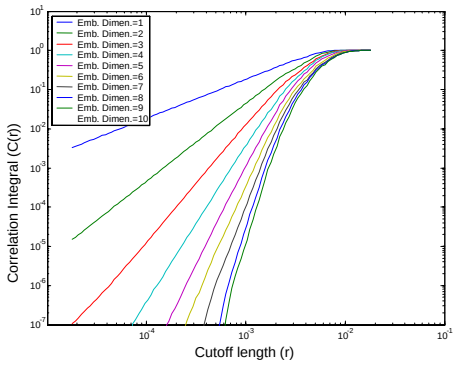

Figure 7. *Plot of log(C(r)) versus log(cutoff length) for a) 3 element box filter applied, b) 9 element box filter applied c) 10 hz box filter in frequency domain applied.*

Table 7. *Correlation dimension for filtered time series.*

TIME SERIES	D_C FROM MEAS. DATA (3 SAMPLE FILTER)	D_C FROM SIMUL. DATA (3 SAMPLE FILTER)	D_C FROM MEAS. DATA (9 SAMPLE FILTER)	D_C FROM SIMUL. DATA (9 SAMPLE FILTER)	D_C FROM MEAS. DATA (10 HZ FILTER)	D_C FROM SIMUL. DATA (10 HZ FILTER)
472s17r512	7.5	9.3	4.6	8.0	4.3	4.2
472s19r512	8.9	7.1	8.2	5.9	3.9	4.4
472s25r512	7.0	7.0	5.3	7.0	3.7	4.9
472s30r512	5.1	5.0	4.7	4.5	**4.5**	4.3
472s31r512	5.4	6.3	4.3	5.4	4.0	4.4
472s37r512	7.2	7.4	7.5	7.3	4.9	4.3
472s38r512	6.1	7.1	5.2	5.8	4.5	4.5
472s43r512	5.3	5.3	5.7	5.3	4.4	3.8
472s30rl	7.2	7.8	8.3	7.8	4.4	4.2
472s31rl	6.8	8.1	7.6	7.3	4.3	4.2

4. Non-linear versus Linear Prediction

The above results argue against the applicability of the chaotic model to sea clutter. However, it can still be speculated that the clutter, or more specifically the underlying texture process, is an inherently non-linear one. While it may not be possible to formulate a generically consistent description such as chaos, it has nevertheless been suggested that it is possible to construct a non-linear predictor which can more accurately predict the value of a clutter return given knowledge of the leading (and possibly trailing) values of the time series in which it is embedded [20]. The improved prediction of underlying texture would allow the performance of a detector to more closely approach that of an ideal CFAR detector [12].

In this section, the relative performance of some selected linear and non-linear predictors for clutter returns are compared. A similar undertaking was performed by Cowper et al. [21] but their study was limited to data sets derived from two sources:

1) wavetank data measured from a radar in a large wavetank facility, and
2) low resolution (150 m resolution) data collected from a stationary land-based radar pointed out to a fixed patch of sea surface.

It might be argued that neither of these sets truly captures the chaotic nature of the sea clutter; the wave tank data may not reproduce the chaotic dynamics that develop in true ocean environments while the low resolution measured sea clutter returns may not adequately capture the chaotic structure that exists in high resolution data. It is well known that sea clutter returns become spikier as the resolution cell of the radar becomes smaller than the length of the swell structure. The sea clutter data examined by Cowper et al. is of such coarse resolution that the underlying swell structure is likely to be heavily filtered. Little improvement would be expected under these conditions by the use of non-linear modelling for an underlying non-linear texture.

Three predictor structures are examined in this section:

1) A simple cell averaging (CA) predictor which predicts the clutter return in the target cell by averaging the value of the returns from cells on either side. This type of predictor is an example of one specific simple form of linear predictor.

2) A generalized linear predictor structure $b = A\lambda$, where A are the values used to form the prediction b. The λ_j constants are determined by a least squares fit to the observations in the learning set. A sensitivity analysis was performed to determine the ideal training sample (learning set) size; little improvement is noted for training sample sizes above 2500. The results reported hereafter are all for a training sample size of 5000.

3) A radial basis function (RBF) non-linear predictor [22]. In this study the basis functions are given as

$$F(\mathbf{x}) = \sum_{j=1}^{n_c} \lambda_j \phi(\| \mathbf{x} - \mathbf{c}_j \|)$$

where $\phi(r) = e^{\frac{-r^2}{\sigma^2}}$ is constructed about n_c number centres (c_j), with the constant σ being determined as a multiple (k) of the average distance (d) between data points (i.e. $k*d$) considered in the fit. $\| \mathbf{x} - \mathbf{c}_j \|$ is the Euclidean norm. The λ_j constants are determined by a least squares fit to the observations in the learning set, $b = A\lambda$, where b are the observations, λ is a vector of length n_c whose jth component is λ_j and A is given by

$$A_{ij} = \phi(\|x_i - c_j\|).$$

The effect of varying n_c and k over ranges of 50 to 300 and 0.0025 to 0.05, respectively, was tested. The results proved relatively insensitive to the value chosen and only the results for $n_c = 150$ and $k=0.01$ are presented.

4.1 Results of Prediction Analysis

Figure 8 illustrates the result of applying the CA predictor to each of the data sets. The Mean Square Error (MSE) is plotted for a variety of lengths of predictor cells. The CA predictor is commonly used to achieve a measure of the underlying power level in clutter with a strong spatial correlation in texture. In application it is common to leave one guard cell on either side of the target cell to ensure that none of the target returns leak into the background estimation. Results are shown for prediction with and without a guard cell.

It is readily apparent from figure 8 that in most cases the best predictability is achieved by use of a 2 cell averager (i.e. one cell on either side) with no guard cell present. This result reflects the fact that the correlation length of the speckle component of the clutter is longer then the time (or distance) between individual measurements. Column 2 of table 8 summarizes the results of figure 8 in which the best (i.e. smallest) mean square error achieved for a CA predictor without a guard cell has been listed. Practically, the operation of a CA predictor without a guard cell could lead to the serious suppression of distributed targets. Typically, a guard cell configuration would be used with correspondingly reduced performance as shown in figure 9. Column 2 of table 9 summarizes the results of figure 9 in which the mean square error achieved for a 12 cell length CA predictor with a guard cell is illustrated. The prediction performance is noticeably reduced.

Column 3 of table 8 also presents the results of using a general linear predictor for an embedding dimension of 10 (i.e. the number of measurements used as input) without a guard cell. The effect of varying the embedding dimension for linear prediction without a guard cell was investigated and little advantage was gained from increasing the embedding dimension beyond 10.

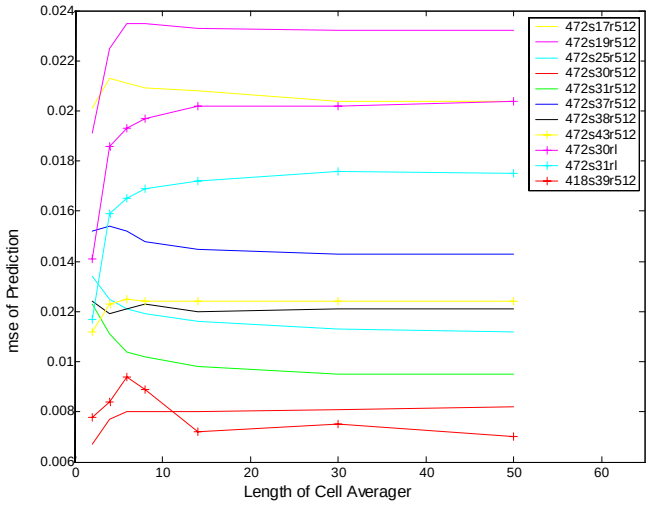

Figure 8: *Mean square error (MSE) of Cell Averaging (CA) predictor with no guard cell versus length of CA for each data set.*

The corresponding results obtained using the RBF non-linear predictor are also listed in column 5 of table 8. As discussed earlier, the *false_nearest* algorithm was used to determine the necessary embedding dimension to reconstruct the attractor of the non-linear chaotic process. The effect of using larger embedding dimensions was investigated. In many cases the larger dimension results in improved performance and rarely in degraded performance although, as with the linear detector, little improvement was noted for embedding dimensions greater than 10. Hereafter only the results for an embedding dimension of 10 are considered unless otherwise noted.

From an examination of columns 3 and 5 of table 8, it is readily evident that the linear and non-linear predictors produce virtually identical results. No performance advantage is evident for either method. It should be noted that sensitivity testing on the RBF predictor indicates that best results are obtained with larger training sets. In all cases prediction was performed using the maximum possible training set size while ensuring that testing was performed on the same segment of the time series for all methods.

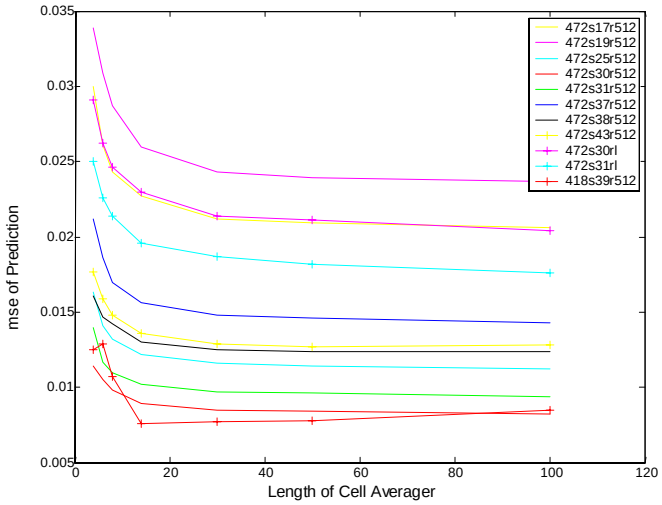

Figure 9: *Mean square error (MSE) of Cell Averaging (CA) predictor with guard cell versus length of CA for each data set.*

Perhaps the most noteworthy fact from the data presented so far is that the simple CA predictor performance exceeds that of both the linear and non-linear predictor. This seemingly surprising outcome is a result of the method in which the points used as input to the predictors are chosen. For the linear and RBF predictor results described above, the input points all lead the time series value we are trying to predict; this contrasts with the CA predictor in which we use values from both the leading and trailing sides of the target cell. If the linear and non-linear attractors are correctly capturing the dominant underlying dynamics it should not make any significant difference how the values are chosen; clearly this is not the case in our test. To further investigate this affect the linear and RBF predictors were rerun with input values chosen to bracket the target cell with and without guard cells (columns 4 and 7 of table 8, and columns 4 and 5 of table 9, respectively). Under the new sampling procedure the linear and RBF predictors display superior results to the CA predictor with a similar number of input samples, however no improvement in performance is noted by using the RBF predictor in place of the linear predictor.

Table 8. *Mean square error (MSE) for CA, linear and RBF predictor without guard cell.*

TIME SERIES	BEST CA MSE WITHOUT GUARD CELL	LINEAR MSE FROM LEADING CELLS & NO GUARD CELLS	LINEAR MSE FROM BRACKET CELLS & NO GUARD CELLS	RBF MSE FROM LEADING CELLS & NO GUARD CELL	RBF MSE FROM LEADING CELLS & NO GUARD CELL +DELAY	RBF MSE FROM BRACKET CELLS & NO GUARD CELL
472s17r512	0.0201	0.0195	0.0179	0.0197	0.0217	0.0176
472s19r512	0.0191	0.0206	0.0175	0.0205	0.0243	0.0171
472s25r512	0.0112	0.0120	0.0118	0.0122	0.0128	0.0114
472s30r512	0.0067	0.0077	0.0064	0.0081	0.0099	0.0065
472s31r512	0.0095	0.0101	0.0102	0.0103	0.0100	0.0104
472s37r512	0.00143	0.0141	0.0133	0.0144	0.0157	0.0134
472s38r512	0.00119	0.0121	0.0111	0.0124	0.0137	0.0111
472s43r512	0.0112	0.0117	0.0103	0.0117	0.0139	0.0101
472s30rl	0.0141	0.0166	0.0124	0.0159	0.0210	0.0111
472s31rl	0.0117	0.0139	0.0102	0.0134	0.018	0.0092
418s39r512	0.0072	0.0078	0.0075	0.0074	0.0135	0.0067

Column 3 of table 9 also shows the best mean square error that was achieved for the CA predictor with a guard cell as shown in figure 9. Unlike the results for no guard cell, in almost all cases the best results with a guard cell are obtained for a CA length of 100 cells (see figure 9). This is a strong indication that the measured returns are stochastic. Once one has moved beyond the region in which the clutter is correlated (i.e. past the guard cells) the best estimate of the mean level is achieved by taking the longest possible ensemble average to minimize statistical error. Tests using increasing embedding dimension for the linear and RBF predictors with bracketing input cells and guard cells (not shown) display a similar improvement.

A final test of the chaotic embedding approach was performed. When reconstructing a chaotic attractor, it is necessary to choose the embedded sample points with a delay spacing that ensures that the full information content of the system is extracted [15]. This delay value was calculated via the *mutual* program discussed earlier. Using the delays listed in table 4, the RBF predictor was rerun with properly spaced embedded values (and leading input samples). The results are presented in column 6 of table 8. Sensitivity testing again showed that no advantage was obtained by increasing the embedding dimension beyond 10. The results of using the delayed embedding are clearly worse then those obtained without delay, inconsistent with a chaotic interpretation.

Table 9. *Mean square error (MSE) for CA, linear and RBF predictor with guard cell.*

TIME SERIES	CA MSE WITH GUARD CELL & CA LENGTH OF 12	BEST CA MSE WITH GUARD CELL	LINEAR MSE FROM BRACKET CELLS WITH GUARD CELLS	RBF MSE FROM BRACKET CELLS WITH GUARD CELLS
472s17r512	0.0227	0.0206	0.0211	0.0216
472s19r512	0.0260	0.0237	0.0237	0.0241
472s25r512	0.0122	0.0112	0.0121	0.0127
472s30r512	0.0089	0.0082	0.0090	0.0101
472s31r512	0.0102	0.0094	0.0097	0.0099
472s37r512	0.0156	0.0143	0.0149	0.0157
472s38r512	0.0130	0.0124	0.0130	0.0132
472s43r512	0.0136	0.0128	0.0131	0.0132
472s30rl	0.0230	0.0204	0.0209	0.0210
472s31rl	0.0196	0.0176	0.0178	0.0179
418s39r512	0.0076	0.0076	0.0095	0.0074

Several conclusions can be derived from the results presented in this section. First, there is no evidence to support a chaotic, or even non-linear, model of the sea clutter as both linear and non-linear detectors produce virtually identical results. Even worse, experiments on the effective training sample size show that a larger training sample is required for the non-linear detector with no improvement in performance. The decreased performance of the RBF predictor when the calculated delay values are used also argues strongly against an underlying chaotic structure. The improved performance of the linear and RBF predictors (for the bracketing input) in comparison with the CA predictor results from their ability to fine tune the linear coefficients which are fixed and equal for the CA predictor. The superior performance of all predictors under no guard cell operation results from their ability to exploit the correlation of the data, an advantage that disappears once the guard cell configuration is introduced. This indicates that the underlying clutter process is a partially correlated stochastic process.

5. Conclusions

No evidence exists for a linear, or more specifically, a chaotic interpretation of sea clutter returns. The invariant measures of correlation dimension per the DML method [8] and largest Lyapunov exponent [18] prove to be ambiguous in their identification of a chaotic process as they produce very similar results for both chaotic and stochastic processes. In addition, it is shown from an examination of the correlation measure versus cut-off length as per the Grassberger and Procaccia [10] method, that measured sea clutter returns produce results incompatible with the chaotic process that were speculated to be responsible.

The concept of an underlying chaotic texture masked by a stochastic speckle component was also examined by filtering but found to suffer the same ambiguities and contradictions as discussed above.

Three linear and non-linear predictors were examined and no performance improvement was noted between linear and non-linear prediction. The behaviour of the predictor outputs under various input configurations were examined and the results from measured clutter returns were found to be most compatible with a partially correlated stochastic process.

References

[1] Leung, H. and Haykin, S.: 'Is there a radar clutter attractor?'. *Appl. Phys. Lett*, 1990, **56**, (6), pp. 593-595.

[2] Leung, H. and Lo, T.: 'Chaotic Radar Signal Processing over the Sea', *IEEE J. Oceanic Engineering*, 1993, **18**, (3), pp. 287-295.

[3] Leung, H.: 'Applying Chaos to Radar Detection in an Ocean Environment: An Experimental Study', *IEEE J. Oceanic Engineering*, 1995, **20**, (1), pp. 56-64.

[4] Haykin, S. and Puthusserypady, S.: 'Chaotic dynamics of sea clutter', *Chaos*, 1997, **7**, (4), pp. 777-802.

[5] Haykin, S.: 'Radar Clutter Attractor: implications for physics, signal processing and control', *IEE Proc.-Radar , Sonar, Navig.*, 1999, **146**, (4), pp. 177-188.

[6] Unsworth, C.P., Cowper, M.R., McLaughlin S., and Mulgrew, B.: 'Re-examining the nature of sea clutter', *IEE Proc.-Radar Sonar Navig*., 2002, **149**, (3), pp. 105-114.

[7] Unsworth, C.P., Cowper, M.R., McLaughlin S., and Mulgrew, B.: 'False detection of chaotic behaviour in the stochastic compound k-distribution model of radar sea clutter', *Proceedings of the 10th IEEE Workshop on SSAP,* August 2000, pp.296-300.

[8] Schouten, J.C., Takens, F., and Van den Bleek, C.M.: 'Estimation of dimension of a noisy attractor', *Phys. Rev. E*, 1994, **50**, pp.1851-1861.

[9] Kennel, M.B., Brown, R., and Abarbanel, H.D.I.: 'Determining embedding dimension for phase-space reconstruction using a geometrical construction', *Phys. Rev. A*, 1992, **45**, pp. 3403-3463.

[10] Grassberger, P. and Procaccia, I., 'Measuring the strangeness of the strange attractor', *Physica D*, 1983, **9D**, pp.189-208.

[11] Haykin, S., Bakker, R. and Currie, B.: 'Uncovering Non-linear Dynamics: The Case Study of Sea Clutter', *Proc. IEEE*, 2002, **90**, (5), pp.860-881.

[12] Watts, S.: 'Radar detection prediction in sea clutter using the compound K-distribution', *IEE Proc.*, Pt. F, 1985, **132**, (7), pp. 613-620.

[13] Blacknell, D., Tough, R.J.A.: 'Parameter estimation for the K-distribution based on [z log(z)]', *IEE Proc. – Radar, Sonar, Navig.*, 2001, **148**, (6) , pp.309-312.

[14] Tough, R.J.A. and K.D. Ward, 'The correlation properties of gamma and other non-Guassian processes generated by memoryless nonlinear transformation', J. Phys. D: Appl. Phys., 1999, **32**, pp.3075-3084.

[15] Parker, T.S. and Chua, L.O., 'Chaos: A tutorial for engineers', *Proc. IEEE*, 1987, **75**, (8), pp.982-1008.

[16] Prof.ir. Cor M. Van den Bleek, *RRChaos Program*, Delft University of Technology, Department of Chemical Process Technology, Julianalaan 136, 2628 BL Delft, The Netherlands, 1992.

[17] R. Hegger, H. Kantz, and T. Schreiber, *Practical implementation of nonlinear time series methods: The TISEAN package*, CHAOS, 1999, **9**, pp. 413.

[18] H. Kantz, *A robust method to estimate the maximal Lyapunov exponent of a time series*, Phys. Lett. A, 1994, **185**, pp.77.

[19] Watts, S., Baker, C.J., and Ward, K.D.: 'Maritime surveillance radar Part 2: Detection performance prediction in sea clutter', *IEE. Proc.*, Pt. F, 1990, **137**, (2), pp.63-72.

[20] Leung, H.: 'Nonlinear clutter cancellation and detection using a memory-based prediction', *IEEE Trans. Aerosp. Electron. Syst.*, 1996, **32**, (4), pp.1249-1256.

[21] Cowper, M.R., Mulgrew, B. and Unsworth, C.P., 'Investigations into the use of non-linear predictor networks to improve the performance of maritime surveillance radar target detectors', *IEE Proc. Radar, Sonar Navig.*, 2001, **148**, (3), pp. 103-111.

[22] S. Haykin, *Neural Networks A Comprehensive Foundation*, Prentice-Hall, Upper Saddle River, 1999.

DOCUMENT CONTROL DATA

(Security classification of title, body of abstract and indexing annotation must be entered when the overall document is classified)

1. ORIGINATOR (the name and address of the organization preparing the document. Organizations for whom the document was prepared, e.g. Establishment sponsoring a contractor's report, or tasking agency, are entered in section 8.)

DEFENCE R&D CANADA - OTTAWA
OTTAWA ONTARIO CANADA K1A 0Z4

2. SECURITY CLASSIFICATION (overall security classification of the document, including special warning terms if applicable)

UNCLASSIFIED

3. TITLE (the complete document title as indicated on the title page. Its classification should be indicated by the appropriate abbreviation (S,C or U) in parentheses after the title.)

Limitations of Non-linear Dynamics in Predicting Sea Clutter Returns (U)

4. AUTHORS (Last name, first name, middle initial)

MC DONALD, MICHAEL K.

5. DATE OF PUBLICATION (month and year of publication of document)	6a. NO. OF PAGES (total containing information. Include Annexes, Appendices, etc.)	6b. NO. OF REFS (total cited in document)
NOVEMBER 2002	38	21

7. DESCRIPTIVE NOTES (the category of the document, e.g. technical report, technical note or memorandum. If appropriate, enter the type of report, e.g. interim, progress, summary, annual or final. Give the inclusive dates when a specific reporting period is covered.)

DRDC OTTAWA TECHNICAL REPORT

8. SPONSORING ACTIVITY (the name of the department project office or laboratory sponsoring the research and development. Include the address.)

DEFENCE R&D CANADA - OTTAWA

9a. PROJECT OR GRANT NO. (if appropriate, the applicable research and development project or grant number under which the document was written. Please specify whether project or grant)	9b. CONTRACT NO. (if appropriate, the applicable number under which the document was written)
3DB29	

10a. ORIGINATOR'S DOCUMENT NUMBER (the official document number by which the document is identified by the originating activity. This number must be unique to this document.)	10b. OTHER DOCUMENT NOS. (Any other numbers which may be assigned this document either by the originator or by the sponsor)
DRDC Ottawa TR 2002-130	

11. DOCUMENT AVAILABILITY (any limitations on further dissemination of the document, other than those imposed by security classification)

(X) Unlimited distribution
( ) Distribution limited to defence departments and defence contractors; further distribution only as approved
( ) Distribution limited to defence departments and Canadian defence contractors; further distribution only as approved
( ) Distribution limited to government departments and agencies; further distribution only as approved
( ) Distribution limited to defence departments; further distribution only as approved
( ) Other (please specify): Canadian Department of National Defence

12. DOCUMENT ANNOUNCEMENT (any limitation to the bibliographic announcement of this document. This will normally correspond to the Document Availability (11). However, where further distribution (beyond the audience specified in 11) is possible, a wider announcement audience may be selected.)

13. ABSTRACT (a brief and factual summary of the document. It may also appear elsewhere in the body of the document itself. It is highly desirable that the abstract of classified documents be unclassified. Each paragraph of the abstract shall begin with an indication of the security classification of the information in the paragraph (unless the document itself is unclassified) represented as (S), (C), or (U). It is not necessary to include here abstracts in both official languages unless the text is bilingual).

The ability to describe sea clutter returns via non-linear, and more specifically chaotic dynamics, is examined. It is shown that the commonly used chaotic invariant measures of correlation dimension and Lyapunov exponent are incapable of uniquely identifying chaotic processes and produce similar results for real sea clutter returns and simulated stochastic processes. The potential existence of an underlying chaotic texture masked by stochastic overlying speckle is examined but found to be inconsistent with the measured properties of the real sea clutter data. Finally the performance of linear and non-linear predictors is tested against the real data but no improvement is found to exist for the non-linear predictor examined in this report with respect to linear prediction performance.

14. KEYWORDS, DESCRIPTORS or IDENTIFIERS (technically meaningful terms or short phrases that characterize a document and could be helpful in cataloguing the document. They should be selected so that no security classification is required. Identifiers such as equipment model designation, trade name, military project code name, geographic location may also be included. If possible keywords should be selected from a published thesaurus. e.g. Thesaurus of Engineering and Scientific Terms (TEST) and that thesaurus-identified. If it is not possible to select indexing terms which are Unclassified, the classification of each should be indicated as with the title.)

SEA CLUTTER
RADAR
CHAOS

Defence R&D Canada

Canada's leader in defence
and national security R&D

R & D pour la défense Canada

Chef de file au Canada en R & D
pour la défense et la sécurité nationale

www.drdc-rddc.gc.ca